DOI: 10.4408/IJEGE.2011-03.B-064

HYDROLOGIC CONDITIONS AND TERRESTRIAL LASER SCANNING OF POST-FIREDEBRIS FLOWS IN THE SAN GABRIEL MOUNTAINS, CA, U.S.A

K.M. SCHMIDT(*), M.N. HANSHAW(*), J.F. HOWLE(**), J.W. KEAN(***), D.M. STALEY(***), J.D. STOCK(*) & W. BAWDENG W. (****)

(*) U. S. Geological Survey, 345 Middlefield Rd., MS-973, Menlo Park, CA, 94025, U.S.A
(**) U. S. Geological Survey, P.O. Box 1360, Carnelian Bay, CA, 96140, U.S.A.
(***) U. S. Geological Survey, P.O. Box 25046, MS-966, Denver, CO, 80225, U.S.A
(****) U. S. Geological Survey, 3020 State University Dr. E., Sacramento, CA 95819, U.S.A.

ABSTRACT

To investigate rainfall-runoff conditions that generate post-wildfire debris flows, we instrumented and surveyed steep, small watersheds along the tectonically active front of the San Gabriel Mountains, California. Fortuitously, we recorded runoff-generated debris-flows triggered by one spatially restricted convective event with 28 mm of rainfall falling over 62 minutes. Our rain gages, nested hillslope overland-flow sensors and soil-moisture probes, as well as a time series of terrestrial laser scanning (TLS) revealed the effects of the storm. Hillslope overland-flow response, along two ~10-m long flow lines perpendicular to and originating from a drainage divide, displayed only a 10 to 20 minute delay from the onset of rainfall with accumulated totals of merely 5-10 mm. Depth-stratified soil-moisture probes displayed a greater time delay, roughly 20- 30 minutes, indicating that initial overland flow was Hortonian. Furthermore, a downstream channel-monitoring array recorded a pronounced discharge peak generated by the passage of a debris flow after 18 minutes of rainfall. At this time, only four of the eleven hillslope overlandflow sensors confirmed the presence of surface-water flow. Repeat TLS and detailed field mapping using GPS document how patterns of rainsplash, overland-flow scour, and rilling contributed to the generation of meter-scale debris flows. In response to a single small storm, the debris flows deposited irregular levees and lobate terminal snouts on hillslopes and caused widespread erosion of the valley axis with ground surface lowering exceeding 1.5 m.

Key words: rainfall-runoff, debris flow, rainfall threshold, terrestrial laser scanning, lidar, wildfire, warning system

INTRODUCTION

Wildfire in the chaparral ecosystem of southern California, U.S.A. along the urban-wildland interface has become a commonplace occurrence and is often ignited by anthropogenic activities (Keeley *et alii*, 1999). In the aftermath of wildfire, increased sediment transport continues into the following winter months and intense rainfall may trigger floods and debris flows that threaten life and property of the communities at the base of steep, burned watersheds. To evaluate these hazards, the U. S. Geological Survey (USGS) and the National Weather Service (NWS), a division of the National Oceanic and Atmospheric Administration (NOAA), have collaborated since 2005 on a demonstration flashflood and debris-flow early warning system for recently burned areas in southern California (NOAA-USGS Debris Flow Task Force, 2005). Goals of this warning system are to predict the timing, location, and relative magnitude of rapid sediment-laden flash floods and debris flows from recently burned drainage basins. Comparisons between forecast and observed precipitation with empirical rainfall thresholds for the initiation of debris flows (e.g., Cannon *et alii*, 2008), as well as maps showing areas susceptible to debris flow (e.g., CANNON *et alii*, 2009) are used to advise the affected populace and civil authorities. In an effort to better constrain the rainfall-runoff conditions leading to initiation of runoff-generated debris-flows and to explore the feasibility of linking hillslope and channel monitoring information with the warning system, we installed ground-based monitoring instruments including rain gages, soil-moisture probes, overland-flow sensors, sediment traps, and erosion pins and conducted repeat terrestrial laser scanning (TLS) in smaller watersheds within six different fires since 2005.

Although the transport and depositional zones of debris flows have been widely studied (Iverson et al., 1997), the hydrologic conditions and topographic locations in which debris flows initiate within burned landscapes remain poorly defined. In contrast to in situ discrete hillslope-scale landslides mobilizing downslope into debris flows (IVERSON *et alii*, 1997), runoff-generated debris flows occur typically in areas of steep topography devoid of vegetation with spatially distributed transport of ample loose sediment (e.g., CANNON *et alii*, 2003; Coe *et alii*, 2008). In burned landscapes, overland flow is commonly observed during relatively low-intensity rainfall events. In contrast, undisturbed forest and chaparral environments with intact organic duff layers above the mineral soil surface have minimal overland flow during low intensity rainfall. In burned areas, soil infiltration capacity is reduced by a complex combination of factors including the removal of organic material, fusing of soil particles into aggregates, fire-induced hydrophobicity, extreme drying of soil, and clogging of pore spaces by ash (e.g., SHAKESBY & DOERR, 2006). This reduction of infiltration capacity can amplify overland flow.

Early recognition of the connection between post-fire conditions and rainfall generating debris flows in the region can be traced to the devastating debris flows and loss of life that occurred in the La Crescenta - Montrose, CA communities in the 1934 New Year's Day Storm (TAYLOR, 1934; EATON, 1936) following fires in 1933. Knowledge regarding debris flows at the time was limited, and for the same event TROXELL & PETERSON (1937) described the event not as debris flows, but as alluvial flows of traction transport with "walls of water" up to 3-m high, although current interpretations support the former. In response to large sediment transporting events such as these, an intricate debris basin system was initiated and managed by the Los Angeles County Dept. of Public Works to capture sediment (http://dpw.lacounty.gov/wrd/sediment/debris_basin_clean_out.cfm). However, the intimate proximity of steep topography and numerous debris basins adjacent to the urban environment dictates frequent and timely maintenance to evacuate trapped sediment. The Station fire burn area, just north of the city Los Angeles, California, U.S.A. was the 10th largest wildfire in California history since 1933, burning a total of 650 km2 of the San Gabriel Mountains from 26 August to 16 October 2009 (http://cdfdata.fire.ca.gov/incidents/). The fire consumed chaparral and mixed coniferous forests within landslide-prone rugged watersheds draining to steep, urbanized alluvial fans. Advisories, watches, and warnings based upon precipitation forecasts provided emergency-response and public-safety agencies information necessary for urgent response decision-making efforts (CANNON *et alii*, 2010). In addition, CANNON *et alii* (2009) presented an emergency assessment of potential debris-flow hazards based upon statisticalempirical models for use by civil authorities. As part of the USGS emergency response, we instrumented sites in an Intensive Research Area (IRA), within watersheds identified by CANNON *et alii* (2009) to have high debris-flow susceptibility. On 12 November 2009 a focused convective rain cell produced debris flows in our IRA. This paper documents our observations, recorded rainfall-runoff data, and changes in topography derived from repeat TLS

STUDY AREA

The San Gabriel Mountains are a prominent, tectonically active range in a Mediterranean climate with thoroughly dissected rugged topography, bordered to the southwest by an urban fringe (Figure 1). The range formed within a large restraining bend of a larger fault system associated with the San Andreas fault, a major continental transform fault. Our IRA field site is located in topography generated by combined displacement from the San Gabriel fault to the northeast, and active thrusting of the Sierra Madre fault to the southwest, with inferred vertical slip rates of 0.5-1.0 mm/yr at the mountain front (LINDVALL & RUBIN, 2003). The field site is underlain by materially weak rock: late Cretaceous hornblende diorite exposed to extensive tectonic shear (SMITH, 1986) that is highly fractured, friable, and chemically weathered. The soil and much

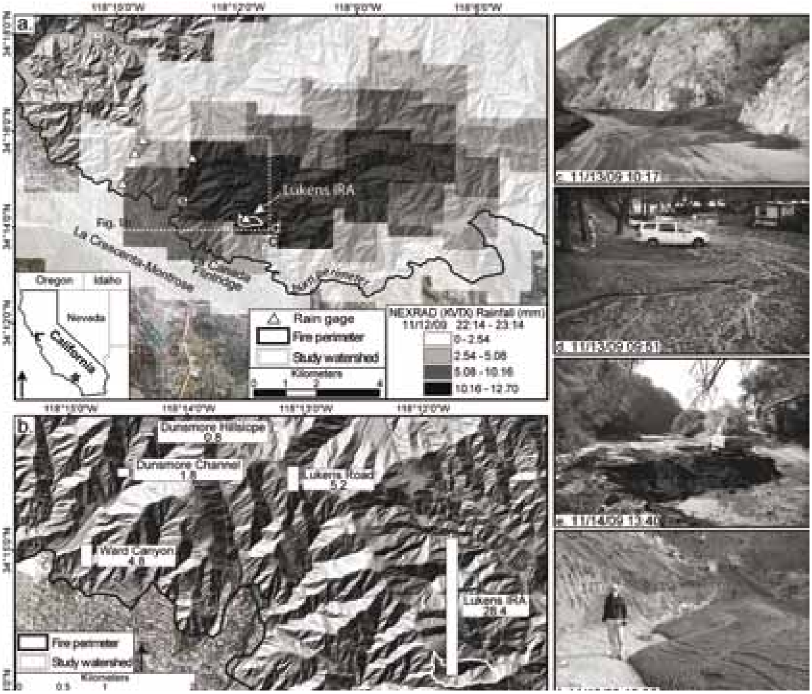

Fig. 1 - Regional study area showing part of the area burned by the Station fire (partial burn perimeter shown as black line) California, U.S.A and Lukens IRA watershed superimposed with November 12th, 2009, rainfall totals from (a) NEXRAD radar data, and (b) cumulative tipping-bucket rain gage totals (mm) with height of bar scaling with rain total [locations denoted by white triangles in (1a)]. Letters c-f indicate the location of the photos from this event: (c) ~1.2-m thick debris flow deposited across the Angeles Crest Highway, (d) U.S. Forest Service vehicle inundated by sediment at the Angeles Crest Fire Station, (e) Mullally Canyon debris basin excavation after reaching full capacity (~7190m3), and (f) debris-flow deposit composed of ample dark, burned material

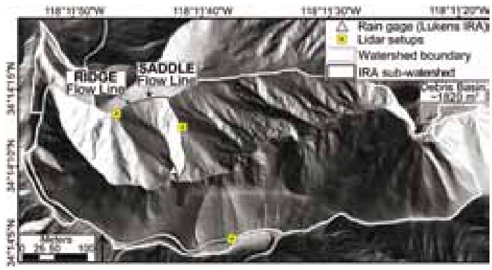

Fig. 2 - Lukens IRA sub-watershed with instrument locations on hillshade derived from airborne lidar. Two surface-flow lines (Saddle and Ridge) were monitored near the drainage divide. Rain gage (Lukens IRA) also denotes location of channel-monitoring array

of the rock exposed at the ground surface had similar strength properties and grain size distributions, and hence abundant unconsolidated sediment was available for transport. The colluvial soils, characteristically less than 0.5 m thick, locally expressed weak pedogenic horizonation. Transport-limited conditions dominated after the fire, prior to the onset of winter rains. Pre-fire vegetation was composed of hard chaparral species assemblages dominated by chamise, ceanothus, mountain mahogany, manzanita, and yucca. Mean annual precipitation in this Mediterranean-type climate ranges between ~700-800 mm/yr (Lavé & Burbank, 2004).

To examine the hydrologic conditions leading to debris-flow generation, we selected a burned, dominantly soil-mantled, unchannelized low-order valley (Lukens IRA, Figg. 1 and 2) in the Station burn area that was hydrologically unaffected by nearby roads. The watershed had convergent steep slopes >30° with ample post-fire ravel filling the valley axes (Figure 3a). Burn severity at the field site was mapped as moderate to high with almost all the ground and shrub vegetation consumed and lower (<10 m) tree canopies burned above the ground. Most woody vegetation <5 mm diameter was consumed by the fire. Relatively planar topography below the convex drainage divide without exposed bedrock, ideal for paired overland-flow and soil-moisture monitoring in the upper reaches of the watershed (Fig. 2). To constrain the timing and hydrologic conditions of coupled hillslope and channel responses, downslope channel monitoring in the same IRA (triangle in Fig. 2) is discussed by Kean & Staley (this volume). Figure 2 illustrates the configuration of our instrumented 12,680 m^2 south-facing, Lukens IRA sub-watershed. The IRA sits within a larger, east-facing 243,035 m^2 watershed with a ~1820 m3 debris catch basin at the Angeles Crest Highway intersection.

METHODS

We measured rainfall-runoff relationships and the geomorphic processes initiating sediment transport, rilling, and debris flows on hillslopes, using rainfall, overland-flow, and soil-moisture monitoring equipment. In the upper watershed of our IRA, we instrumented 10-m long segment of two surface-water flow lines ("Ridge" and "Saddle" in Figure 2), with soil-moisture probes under the ground surface placed near overland-flow sensors (OFS) to detect whether surface-water flow generating mechanisms were saturation driven and/or Hortonian. The soil-moisture probes were installed >1.5 m to <6.1 m away from the OFS placed on the ground surface. To minimize disruption of surface-water flow paths during the digging of soil pits, probes were not installed directly underneath the OFS. Soil-moisture probes were installed by digging three pits to identify soil horizons, were inserted roughly parallel to the ground surface, and were vertically stratified. We installed a total of 6 OFS (USGS-developed closed loop voltage conducting circuits developed by John Moody, USGS, personal communication, Figure 4) and 4 soil-moisture probes used to infer volumetric water content (Decagon ECH20 EC-5 sensor based on electrical conductivity) on the Ridge flow line, and 5 OFS and 3 soil-moisture probes on the Saddle flow line (Fig. 4). Rainfall was recorded by an Onse RG3-M tipping-bucket rain gage (0.2 mm/tip). All instruments were installed prior to rainfall and data was retrieved the day following the event. At this site, and within other catchments of suspected high debris-flow susceptibility in the Station burn area, instrumental records were recorded by either non-telemetered, temporally synchronized data loggers or in near realtime telemetered data streams (e.g., http://landslides.usgs.gov/monitoring).

We also surveyed high-resolution (sub-cm-scale laser point spacing) topography using TLS of the entire Lukens IRA subwatershed on 12 and 13 November 2009, only hours prior to and immediately following the storm, to record the temporal and spatial distribution of surface erosion by overland flow and sediment transport by debris flows. Bare-earth digital elevation models (DEMs) were generated from scans obtained from three laser instrument set ups on 12 November and two set ups on 13 November. The raw data were processed in PolyWorks and TerraScan to remove vegetation. Bare-earth DEMs, with a 0.02-m cell spacing, were krigged in Surfer and imported into ArcGIS to define the spatial projection, merged if tiling was necessary due to large file sizes, and georeferenced using differential, post-processed kinematic GPS locations of four fixed location monuments visible in the scans. Topographic and hydrologic routing analyses of TLS DEMs were performed using ArcGIS. Post-storm observations of runoff characteristics were located using post-processed, differential kinematic GPS. We identified evidence of debris-flow generation by visually inspecting deposits for matrix support, a lack of stratification, and an absence of textural sorting. We then walked upslope from identified debris-flow deposits, tracing evidence to its farthest upslope extent, and examined the ground surface for indications of triggering mechanism.

RESULTS

Prior to the onset of 12 November 2009 rain, sediment transport in the IRA watershed was dominated by post-fire dry ravel. Beginning on 6 October 2009, we observed periodically active sediment transport of dry-ravel material on the planar and convex portions of the topography and accumulating into the convergent valleys (Fig. 3a). The dry, principally unconsolidated colluvium that had been stored upslope of vegetation, which acted as local sediment storage dams, began moving downslope from topographically planar and divergent hillslopes toward convergent val-

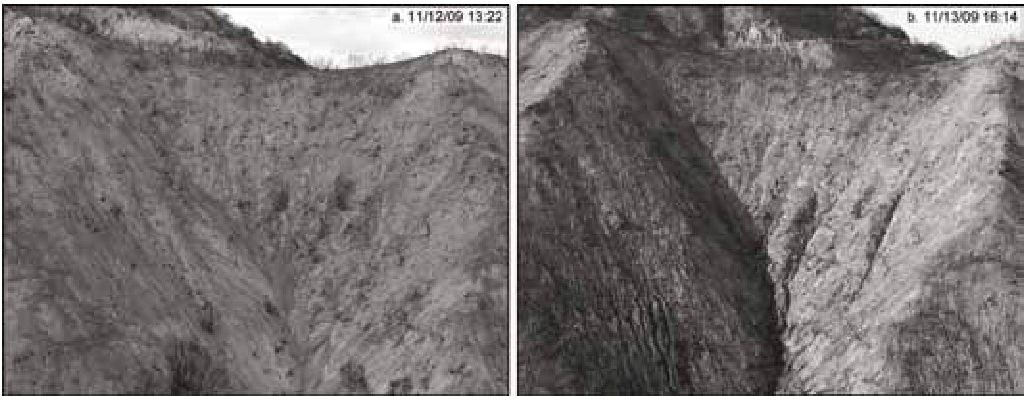

Fig. 3 - Photographic view to North of upper portion of Lukens IRA sub-watershed before rainfall (a), and after (b); times in upper right

Fig. 4 - Before (a) and after (b) photographs of the overland-flow sensors (Saddle flow line). Note the rainsplash-induced pockmarks and cm-scale width semicontinuousrill network in (b) extending to within 0.5-2.0 m of the diffuse convex drainage divide

leys following vegetation removal by wildfire. Prior to rainfall, all pre-fire deposits in the valley axis were uniformly covered by recent post-fire dry-ravel deposits (Fig. 3a).

STORM RAINFALL AND SEDIMENT TRANSPORT

Only a few hours following site installation and TLS surveying, at ~22:00 (Pacific Standard Time: PST) 12 November 2009, a spatially restricted convective cell produced a total of 28.4 mm of precipitation during a 62 minute period over our monitoring site (Figg. 1 and 5). The resulting sediment transport and debris flows filled catch basins at watershed outlets (e.g., Fig. 1e). Some catch basins were filled beyond capacity, causing debris to overtop structures and spill over onto roads and into residential properties, leaving deposits ~0.6-1.2 m thick. Numerous flows also blocked both lanes of the Angeles Crest Highway (e.g., Fig. 1c), but some stopped abruptly upon exiting steep, confined valleys (Figure 1f). Figures 3 and 4 illustrate how surface morphology was altered at the site by runoff-induced surface flow in response to this short, intense rainfall burst.

An empirical intensity (I) - duration (D) threshold curve derived prior to the storm (Cannon *et alii*, 2010) indicated that for durations of 30- and 60-minutes, precipitation greater than 15 and 13 mm/hr respectively, would produce several debris flows over a localized area. During the 12 November storm, however, the peak 30- and 60- minute intensities measured by the rain gage in the IRA exceeded 60 and 30 mm/hr respectively. Figures 1 and 5a depict how cumulative rainfall from the storm dramatically varied across the

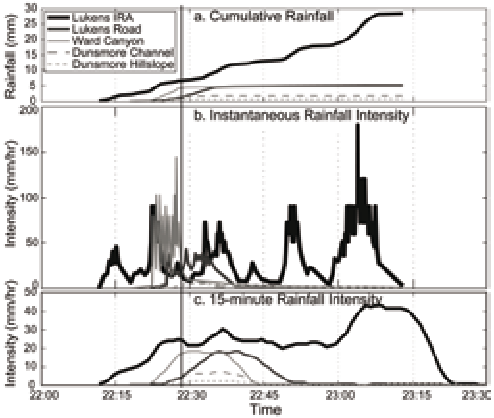

Fig. 5 - Rainfall (a: cumulative, b: instantaneous intensity, and c: 15-minute normalized intensity) recorded at 5 gages located in Figure 1. Vertical line denotes debris-flow discharge peak in channel monitoring data at Lukens IRA outlet

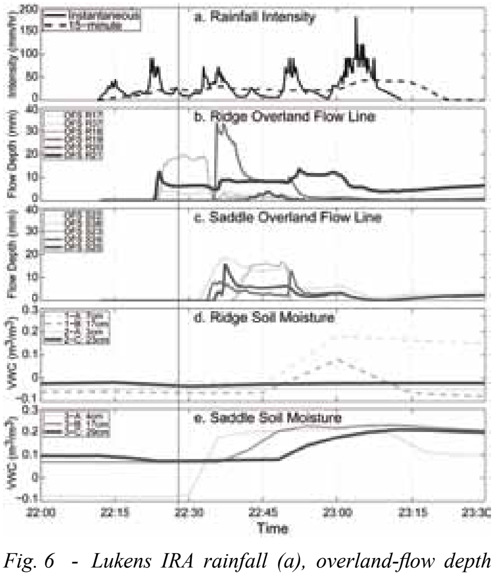

Fig. 6 - Lukens IRA rainfall (a), overland-flow depth (b: Ridge flow line, c: Saddle flow line), and volumetric water content, VWC (d: Ridge flow line, e: Saddle flow line). Lines in (b) and (c) become darker and thicker with increasing distance from ridge top. In (d) and (e) lines become darker and thicker with increasing depth below the ground surface. Numbers (1, 2, and 3) in (d) and (e) indicate different soil-moisture pits, letters (A, B, and C) indicate the soil horizon where probes were situated and depth below ground surface. Vertical line denotes debris-flow discharge peak in channel monitoring data at Lukens IRA outlet

mountain front, with the highest totals recorded at the Lukens IRA, and how the NEXRAD radar data under-represented the rainfall totals. According to the National Weather Service, precipitation models did not accurately predict the location or total rainfall of the storm, and satellite imagery did not adequately characterize rainfall totals during the storm (NWS WFO Memorandum, Eric Boldt, personal communication) and as a result, no public advisory was issued.

TIMING OF RAINFALL, OVERLAND FLOW, SOIL MOISTURE,AND DEBRIS FLOW

Figures 5 and 6 reveal a short response time between the onset of rainfall and the inception of measurable overland water flow. Overland-flow response along the Saddle and Ridge flow lines, originating from the drainage divide, was delayed only by 10 to 20 minutes after the onset of rainfall; accumulated rain totals during this time were merely 5-10 mm. The Ridge line sensors reacted first, preceding the first Saddle line response by more than 8 minutes, likely a reflection of topographic location within a larger contributing drainage area, higher gradient of contributing area, and possibly differences in hydrologic response of surficial materials. Analysis of our TLS-derived topography showed that the farthest upslope sensor on the Ridge line had a drainage area of ~1-2 m^2, compared to <1 m2 on the Saddle line. Within an individual flow line there was no discernable downslope increase in recorded flow depth over the 10-m long interval. Post-storm erosional paths were observed to be irregular, concentrated within anastomosing networks (Fig. 4) that possibly varied in position and discharge throughout the storm.

Relative to the rapid responses of the Ridge line overland-flow sensors, responses of depth-stratified soil-moisture probes displayed a greater delay after rainfall onset, as much as 20-30 minutes (Fig. 6). Only one soil-moisture probe, the shallowest inserted at 4-cm below ground surface in the Saddle line (Figure 6e, probe 3-A), displayed a response beginning at about the same time as the first Saddle-line overland flow sensor response. This soil-moisture probe did not appreciably respond until 7 mm of rain had fallen, 18 minutes after the onset of rainfall. Initial surface runoff, then, was likely Hortonian in behavior, and occurred during dry soil-moisture conditions. Early storm rain intensities likely surpassed the infiltration capacity of the near-surface hydrophobic A-horizon soil, a trait supported by infiltration experiments. In addition, droplet tests at random locations to identify the presence of hydrophobic soils revealed widespread and somewhat laterally continuous hydrophobicity.

In soil-moisture soil pits 1 and 3, increased volumetric water content progressed downward, consistent with top-down infiltration. Shallow probes responded prior to those inserted at deeper depths within the same soil pit (Fig. 6). The deepest probe (29-cm depth in saprolite, pit 3) responded 36 minutes after rainfall began with over 13 mm of accumulated rain. This pattern was not observed at pit 2, where no response was recorded, perhaps reflecting the effectiveness of hydrophobicity near the ground surface impeding local vertical infiltration.

We constrained the timing of sediment transport using data from overland-flow sensors located on planar hillslopes just downslope of the drainage divide, and from the channel monitoring discharge array. Channel monitoring instruments, located at the watershed outlet (12,680 m^2 drainage area denoted by the Lukens IRA rain gage in Fig. 2), recorded an abrupt, pronounced discharge peak, presumably of debris-flow origin, after 16 minutes of rainfall with a total accumulation of merely 6.5 mm (vertical line on Figures 5 and 6) (Kean & Staley, this volume). At this time, only four of the eleven overland flow sensors recorded measurable surface water and the soil-moisture probes had not yet demonstrated significant infiltration leading to increase soil moisture. Based on the stratigraphy of deposits at the Lukens IRA watershed outlet, we suggest the following sequence of transport events: an initial wave of debris-flow transport that was over-printed by more spatially widespread fluvial (traction, saltation, and suspension) transport later in the storm in response to higher rainfall intensities. Debrisflow deposits in the valley axis and on the hillslopes were truncated and appeared incised by later stage overland flow and fluvial transport. As such, the majority of the response recorded after 22:30 by the overland-flow sensors likely represents runoff contributing to the post-debris-flow traction transport.

TERRESTRIAL LASER SCANNING AND FIELD OBSERVATIONS

We scanned the Lukens IRA topography with a terrestrial laser, hours preceding and following the rainfall-runoff event, to characterize watershed morphology and to document magnitudes and spatial patterns of erosion and deposition. These TLS surveys revealed that the average gradient of the watershed was 39°, the maximum gradient was 88° in an area of exposed bedrock, and the relief from the drainage divide at the overland-flow lines was ~112- 118 m, with a maximum of 130 m. Pre-storm topography reflected a dominantly soil-mantled landscape with smooth, planar hillslopes on the west flank of the north-northwest trending, valley axis, an east flank with more incised bedrock-controlled sub-basins, and an unchannelized valley axis filled principally by dry-ravel accumulation (Fig. 3a). Our post-storm survey depicted topography with a much higher drainage density and a well-incised valley axis (Fig. 3b). Almost the entire area expressed evidence of surface runoff by the ubiquitous presence of small rills, but the incision depth of many rills on the hillslopes was generally <5 cm. Field observations following the event indicated that the granular materials below depths of ~10 cm principally remained dry. We estimated ground-surface elevation change by differencing bareearth DEMs generated from the 12 and 13 November surveys (Fig. 7). Although much of the survey extent exhibited little to no vertical (within 5 cm) ground surface change in the upper third of the Lukens IRA watershed, pronounced incision occurred at a smaller number of larger rills and valley incision exceeded 1.5 m the main previously unchannelized valley axis. Recently exhumed materials on the valley floor consisted of colluvium, post-fire dryravel deposits exposed on valley walls, bedrock, and saprolite. Hence, the sediment sources entrained in the debris flows were a combination of material stored in the channel before the fire, postfire dry-ravel deposits, and minor bedrock excavation. Excavations deeper than 1 m into sediment stored in the valley axis appeared discontinuous and probably were limited by structurally controlled bedrock depressions. On the previously smooth, planar western watershed flank, overland flow incised widespread sub-parallel, levee-lined rills. Levee-bounded tracks that were not incised into hillslope materials, with base levels of the pre-existing surface, were also observed. Numerous sub-meter wide and decimeter-thick debris flows deposited over ravel deposits or white ash and char horizons.Hillslope debris-flow deposits, incised by later stage fluvial erosion, ranged up to 3-m in length and were characterized by non-stratified, non-imbricated, matrix-supported coarse and fine-gravel

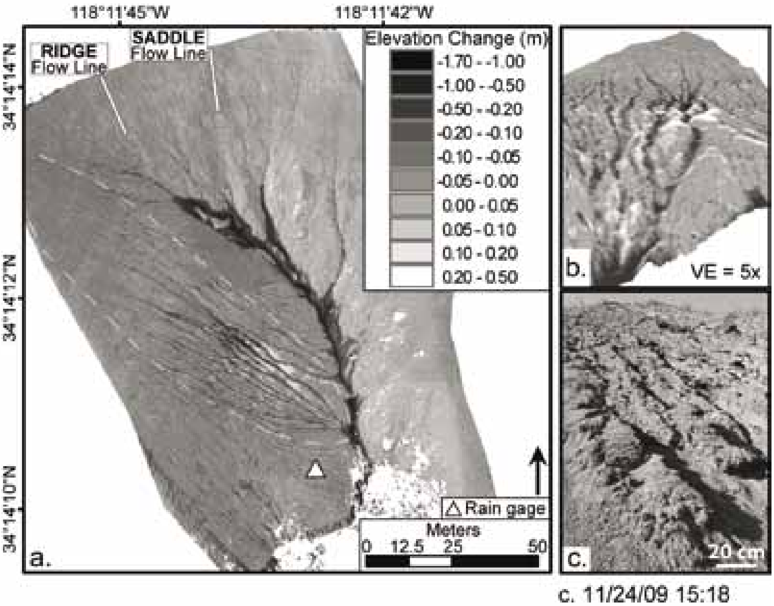

Fig. 7 - Surface elevation change between terrestrial laser scans (11/13/09-11/12/09). Negative values indicate lowering, and positive values indicate aggradation. (a) Lukens IRA watershed, (b) view upslope from valley axis [area defined by white dashed polygon in (a), with 5x vertical exaggeration] highlighting lobate terminal snouts, shown in (c) photograph of debris-flow deposits on gradients of ~33°

clasts mantled by fine silt; low-density char and unburned organic material was uniformly disseminated throughout the deposits. Hillslope debris-flow deposits on the western flank of the watershed deposited upslope of the primary valley axis. Topographic changes to the western flank are interpreted to have progressed in the following sequence: the levee-lined tracks not incised into hillslope materials and decimeter-scale debris-flow deposits were incised by later stage levee-lined rills generated by overland surface flow. This later stage incision exhumed dry material to depths of 0.6 m, far below the observed wetting front depths of ~10 cm, and hence their formation is consistent with rill formation by fluvial transport. Although some of the drainage flow paths generated by the storm were sinuous and anastomosing near the ridge top (e.g., Fig. 4b), the hillslope-scale drainage pattern was generally linear, sub-parallel paths within more planar topography (e.g., Fig. 7).

Employing differential, post-processed kinematic GPS surveys, we mapped and compared geomorphic transport boundaries within the pre- and post-storm TLS-derived DEMs. Rainsplash and unchannelized sheetflow evidence was limited parallel to the ridge top axis. Surface-water flow accumulations derived from the 13 November TLS data indicate that upslope heads of the levee-lined rills had contributing drainage areas of <1 m2 whereas debris flows were identified in >25-30 m^2 drainage areas.

From our TLS surveys and field observations, we interpreted that surface erosion and debris flows were generated by the following influences: i) sediment accumulation by post-fire, pre-rain dry-ravel processes acting under the combined influence of gravity and wind that loaded valley axes with loose sediment and then ii) relatively small rainfall amounts promoted the rapid development of shallow overland-flow drainage networks into both colluvial soil and recently-transported ravel deposits. We interpreted the remaining, somewhat scant, evidence of debris-flow generation by walking upslope from debris-flow deposits, tracing evidence to the farthest upslope extent. Much of the evidence indicates that the initial surface flow did not appreciably incise, but rather flowed over a primarily dry ground surface and entrained sediment by traction and saltation with additional contributions from small, cm-scale (<10 cm high scarps) landslides. Scarps contained threadlike broken roots. These small Coulomb-style slab failures were likely episodicand punctuated sediment concentrations within the surface-water flow. We suspect these onslope debris flows depicted in Figure 7c were generated, at least in part, by a process similar to that elaborated by Wells (1987) where small Coulomb-style failures on the scale of centimetres to decimetres wide form above a water repellent layer. These failures cause material to slide downslope and mobilize into debris flows which in turn plows a path through the granular sediment and deposits steep-faced lobate snouts downslope of levee-bounded tracks (Fig. 7c). Local bedrock exposures routing water to newly formed drainage networks may have also contributed to "fire-hose" mechanism generated debris flows. Watershed-averaged surface elevation change attributable to this individual storm, calculated from the difference grid depicted in Figure 7a, was: maximum 1.10 m, minimum -1.68, average -0.03, and standard deviation ± 0.12 m. The associated volume of material represented by this lowering is 336 m^3. Average lowering within the valley axis of -0.53 m (standard deviation ± 0.29 m) resulted in an estimated volume of 232 ± 127 m^3, hence the majority (~70%) of the sediment volume removed was derived from post-fire dry-ravel accumulations and pre-fire sediment stored in the valley axis.

DISCUSSION AND SUMMARY

Using instrumental monitoring of rainfall and runoff, bare-earth model DEMs developed from repeat laser scanning of topography, and field mapping assisted by differential kinematic GPS, we documented how spatial patterns of rainsplash, overland-flow scour, and rilling changed in response to a localized storm that generated meter-scale debris flows. These flows deposited both irregular levees and lobate terminal snouts on portions of the hillslope and at the watershed confluence. The majority of the erosion by volume (~70%) occurred by excavation of post-fire dry-ravel accumulations and older colluvial soil in the previously unchannelized valley axis with average ground surface lowering >0.5 m. Rainsplash and sheetflow erosional processes were spatially restricted along the gentler convex ridge top, whereas channelized flow processes that generated incisional levee-lined rills and non-incisional levee9 bounded tracks leading to debris-flow deposits were widespread. Post-storm observations indicated that rills (~5-20 cm wide) formed primarily where loose, granular material, post-fire ash, and charcoal deposits remained and extended to within 0.5-2.0 m of the drainage divide. Based on our two monitored surface-flow lines, it appears that upslope contributing drainage area influenced the location and timing of flow generation, with the steeper, larger drainage area responding first.

Geomorphic sediment transport processes in our study area varied spatially, as well as temporally during a single storm. The disparity in timing and spatial extent of both soil moisture and overland-flow responses highlights the complications imposed by rapid runoff from both colluvial soil expressing varying degrees of hydrophobicity and lower permeability bedrock exposed at surface. Overland-flow sensors and soil-moisture probes indicated that the colluvial soil was unsaturated prior to and during the initial pulses of overland flow and debris-flow transport. At the time of recorded passage of a debris flow at the Lukens IRA watershed outlet, only four of the eleven overland flow sensors recorded measurable surface water and the soil-moisture probes had not yet demonstrated measurable increases. Within 15-20 minutes after the onset of rainfall, there was rapid development of surface runoff leading toincision and redistribution of sediment. Although sediment transport rates should be ultimately controlled by rainfall intensity, duration, and subsequent available water discharge, the timing of the debrisflow peak at the Lukens IRA watershed outlet occurred during a lull in rainfall following two initial higher intensity rainfall episodes totaling just over 6 mm in sixteen minutes. This debris flow was triggered by rainfall that exceeded previously established empirical thresholds for post-fire debris-flow initiation (Cannon *et alii*, 2010). The highest recorded rainfall intensities followed the occurrence of debris flows. Field evidence indicates that initial debris-flow deposits were over-printed by later fluvial incision, at both the hillslope and higher-order valley scales.

During the height of the storm, when overland-flow processes likely dominated, the greatest volumetric water content in the colluvial soil was uniformly less than 0.2 m^3/m^3, with one soilmoisture pit showing no increase in volumetric water content during the duration of the storm. Probe responses in the two pits exhibiting moisture response were consistent with top-down, infiltrationlimited water migration. Field observations following the event indicated that the granular materials below depths of ~10 cm principally remained dry in agreement with our soil-moisture probe responses. The presence of incisional rills into the underlying dry material at depths >10 cm is likely consistent with rill formation by fluvial transport. These observations suggest that instrumental monitoring could be used to improve realtime warning systems, but lead times for advisories after the onset of rainfall would remain short in steep, small drainage area basins and thus the operational aspect of issuing advisories with such short lead times may be untenable.

Even with instrumental records, topographic surveys, and firsthand observations immediately following the storm, it remains unclear if the resulting drainage network formed in place or if rill heads migrated upslope over time. Nor is it readily apparent why small debris flows deposited on moderately steep gradients of 30- 35°. A combination of downslope dewatering of the granular material, slight decreases in the gradient of the surface traversed, increased basal friction, and/or a change in ground surface material from colluvial soil to post-fire ravel deposits may have contributed to deposition on such gradients. As the lobate debris-flow snouts stratigraphically overlie widespread post-fire ravel aprons located on lower reaches of hillslopes, it is possible that a combination of slight decreases in downslope gradient coupled with a more permeable bed material may have contributed to deposition. Although some debrisflows deposited on hillslopes, others traversed the primary valley axis and left deposits at the watershed outlet. These deposits were subsequently re-entrained by and incised into by traction-dominated, surface-water transport later in the storm.

ACKNOWLEDGEMENTS

Land access was made possible by the courteous and professional employees of the Cities of Pasadena (Lisa Derderian & Shawn Kwan) and Glendale, CA Parks, Recreation & Community Services (specifically Jeff Weinstein, David Ahern, & Russ Hauck). Sandra Bond (USGS) provided invaluable TLS data processing support. The USGS Landslide Hazards and National Cooperative Geologic Mapping Programs provided funding for this research. We thank Sue Cannon and Mark Reid for thorough and insightful reviews.

REFERENCES

Cannon S.H., Gartner J.E., Parrett C., & Parise M. (2003) - *Wildfire-related debris-flow generation through episodic progressive sedimentbulking processes, western USA.* In: Rickenmann D. & Chen C.L., eds. *Debris-Flow Hazards Mitigation: Mechanics, Prediction, and Assessment*: Davos, Switzerland, Millpress, 71-82.

Cannon S.H., Gartner J.E., Wilson R.C., Bowers J.C. & Laber J.L. (2008) - *Storm rainfall conditions for floods and debris flows from recently burned areas in southwestern Colorado and southern California.* Geomorphology, **96**: 250-269.

Cannon S.H., Gartner J.E., Rupert M.G., Michael J.A., Staley D.M. & Worstell B.B. *(2009) - Emergency assessment of postfire debris-flow hazards for the 2009 Station fire, San Gabriel Mountains, southern California.* U.S. Geological Survey Open–File Report 2009-1227. (http://pubs.usgs.gov/of/2009/1227/).

Cannon S.H., Boldt E.M., Kean J.W., Laber J.L. & Staley D.M. (2010) - *Relations between rainfall and postfire debris-flow and flood magnitudes for emergency-response planning, San Gabriel Mountains, southern California.* U.S. Geological Survey Open–File Report 2010- 1039. (http://pubs.usgs.gov/of/2010/1039/).

Coe J.A., Kinner D.A., & Godt J.W. (2008) - *Initiation conditions for debris flows generated by runoff at Chalk Cliffs, central Colorado.* Geomorphology, **96:** *270-297.*

DiBiase R.A., Whipple K.X., Heimsath A.M. & Ouimet W.B. (2010) - *Landscape form and millennial erosion rates in the San GabrielMountains, CA.* Earth and Planetary Science Letters, **289:** *134-144.*

Eaton E.C. (1936) - *Flood and erosion control problems and their solution.* Proceedings of the American Society of Civil Engineers, **62**(8): 1302–1362.

Iverson R.M., Reid M.E. & LaHusen R.G. (1997) - *Debris flow mobilization from landslides.* Annual Reviews of Earth and

Planetary Sciences, **25**: 85-138.

Kean J.W. & Staley D.M. (this volume) - *Direct measurements of post-fire debris-flows: examples from monitoring efforts in southern California 1832.*

Lavé J. & Burbank D. (2004) - *Denudation processes and rates in the Transverse Ranges, southern California: Erosional response of a transitional landscape to external and anthropogenic forcing.* Journal of Geophysical Research, 109: F01006, doi:10.1029/2003JF000023.

Lindvall S.C. & Rubin C.M. (2003) - *Slip rate studies along the Sierra Madre-Cucamonga fault system using geomorphic and cosmogenic surface exposure age constraints.* Collaborative research with Central Washington University and William Lettis & Associates, Inc. U.S. Geological Survey final report NEHRP External Grant Award Number 03HQGR0084. (http://earthquake.usgs.gov/research/external/reports/03HQGR0084.pdf)

NOAA-USGS Debris Flow Task Force (2005) - *NOAA-USGS debris-flow warning system - Final report.* U.S. Geological Survey Circular 1283. (http://pubs.usgs.gov/circ/2005/1283/).

Shakesby R.A. & Doerr S.H. (2006) - *Wildfire as a hydrological and geomorphological agent.* Earth-Science Reviews, **74**: 269-307.

Smith D.P. (1986) - *Geology of the north half of the Pasadena quadrangle, Los Angeles County, California.* Division of Mines and Geology Open File Report, OFR 82-10LA, map scale 1:12,000.

Spotilla J.A., House M.A., Blythe A.E., Niemi N.A. & Bank G.C. (2002) - *Controls on the erosion and geomorphic evolution of the San Bernardino and San Gabriel Mountains, southern California.* In: Barth, A., ed., Contributions to Crustal Evolution of the Southwestern United States: Boulder, Colorado, The Geological Society of America Special Paper **365**: 205–230.

Taylor C.A. (1934) - *Debris flow from canyons in Los Angeles County flood.* Engineering News-Record, **112**: 439-440.

Troxell, H. C. & J. Q. Peterson (1937) - *Flood in La Cañada Valley California, January 1, 1934.* U. S. Geological Survey Water-Supply Paper 796-C: 98.

Wells W.G. II *(1987) - The effects of fire on the generation of debris flows in southern California.* In: Costa J.E. & Wieczorek, G.F., eds., *Debris flows/avalanches: process, recognition, and mitigation*. Boulder, CO, The Geological Society of America, Reviews in Engineering Geology, **VII**: 105-114.

